© Indian Academy of Sciences

CrossMark

Effects of conjugation on the properties of alkynylcarbazole compounds: experimental and theoretical study

**HUSSAIN AHMED ABRO[1,2], BAODONG ZHAO[2], WEIXIANG HAN[2], XIAOYU MA[2]
and TAO WANG[1,2,*]**

[1]State Key Laboratory of Chemical Resource Engineering, College of Science, Beijing University of Chemical Technology, Beijing 10029, People's Republic of China
[2]Department of Organic Chemistry, College of Science, Beijing University of Chemical Technology, Beijing 10029, People's Republic of China
*Author for correspondence (wangtwj2000@163.com)

Abstract. Four novel dyes containing alkynylcarbazole, namely, 2-((9H-carbazol-3-yl)ethynyl)-9-ethyl-9H-carbazole, 3,6-bis((9-ethyl-9H-carbazol-2-yl)ethynyl)-9H-carbazole, 3-(phenylethynyl)-9H-carbazole and 3,6-bis(phenylethynyl)-9H-carbazole, were synesized on the basis of single and double substitutes by following the Sonogashira coupling method. The synthesized dyes were then assessed as novel photosensitizers in visible-light photopolymerization to evaluate the effects of conjugation on the properties of aromatic compounds. A comparison between UV–vis and TD/DFT electron transition spectra shows that $\lambda_{\max}$ in theoretical ultraviolet spectra matched well with the experimental spectra; every conjugated alkynylcarbazole dye exhibits a wide absorption band in the range of 300–400 mm. Moreover, conjugation enhancement by switching carbazoleacetylene moieties caused a red shift in the absorption bands. The theoretical study showed that the maxima λ of these molecules ranged from ∼330 to 370 mm, corresponding to $\pi \rightarrow \pi^*$ and $n \rightarrow \pi^*$ electron transitions. Fluorescence spectroscopic data show that the strongest emission peaks exhibit a red shift because of the addition of conjugated acetylene groups. A combination of alkynyl dyes and iodonium under a halogen lamp atmosphere by visible-light photopolymerization displayed a positive response to the cationic polymerization of bisphenol-A epoxy resin A and free-radical polymerization of tripropylene glycol diacrylate.

Keyword. Synthesis; alkynylcarbazole; DFT calculations; photosensitizers; photopolymerization.

1. Introduction

Photopolymerization is no doubt a renowned and expedient method broadly used in many industrial applications. Application of photopolymerization as a visible-light-induced photoinitiating system is considered as feasible because of its astonishing advantages such as squat energy feasting, diminutive ecological contamination, swift polymerization level, inconsequential polymerization temperature and broad flexibility [1,2].

Previous research studies have revealed that photosensitizers can enhance the efficiency of visible-light photoinitiating systems. Several groups of scientists in the field of photopolymerization have proposed that their work offers excellent success ratios by introducing photosensitizers, monomers, de-escalation compounds and photoinitiators under LED and halogen lights [3–7].

Structural variation can affect the properties of synthetic compounds. In visible-light photoinitiating systems, increased conjugation in the structure of photosensitizers can cause an increasing absorption in the visible-light range. A conjugated compound, carbazole, is known for its electron-donating properties and has been accredited as a good photosensitizer for iodonium salts in photopolymerization [8–10]. Moreover, application of dyes containing carbazole moiety-based photoinitiators was also appreciated in photopolymerization under LED and halogen lights [11–13].

DFT calculations and simulations unlocked a new era of research that help scientists obtain the best expected results before any physical/experimental treatment. Thus, the literature shows excellent work on several dye compounds, photosensitizers and coating materials by using several methods, such as DFT, TD/DFT and vertical excitation, to evaluate the methodology [14–19].
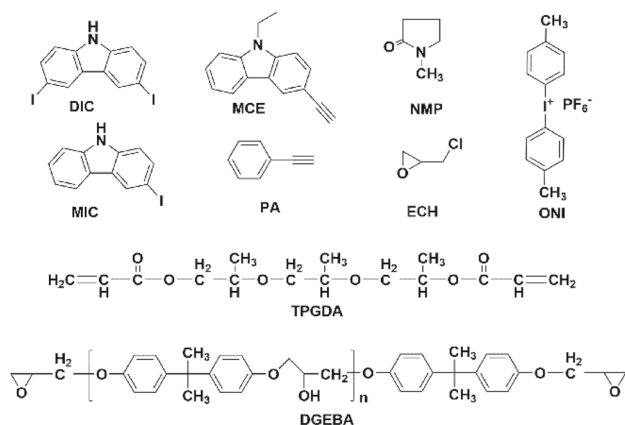
Figure 1. Structures and abbreviations of composites used in this study.

To obtain novel photosensitizers in visible-light photopolymerization and to evaluate the effects of conjugation on the properties of compounds containing carbazole, four novel dyes containing alkynylcarbazole, MEC, DEC, MPC and DPC were synthesized. Their photophysical properties were studied by experiment and DFT calculation. The combinations of alkynyl dyes and iodonium salts were evaluated in the cationic polymerization of bisphenol-A epoxy resin A and free-radical polymerization of tripropylene glycol diacrylate (TPGDA) under a halogen lamp atmosphere.

2. Experimental

2.1 *Materials*

Phenylacetylene (PA), epichlorohydrin (ECH) and *N*-methylpyrrolidone (NMP) were obtained from Beijing Chemical Works (Beijing, China). TPGDA (from Eternal Chemical Co. Ltd, Zhuhai, China) and epoxy resin A (DGEBA, from Jiangsu Sanmu Company, China) were chosen as the monomer and oligomer. 3,6-Diiodo-9*H*-carbazole (DIC), 3-iodo-9*H*-carbazole (MIC) and 9-ethyl-3-ethynyl-9*H*-carbazole (MCE) were synthesized following the literature [20–22]. Figure 1 shows the structures and abbreviations of compounds applied in this work.

2.2 *Characterization*

Melting points (MP) of the composites were obtained by using an XT-4 microscopic MP tool. ^{1}H NMR and ^{13}C NMR spectra were chronicled by using a Bruker AV400 (400 MHz) NMR spectrometer. HRMS extents were obtained by using an LC/MSD TOF mass spectrometer. The IR spectroscopy test was done by using a Nicolet Avatar 370 MCT with the use of KBr pellets. A UV-5200 (UNICO) UV–vis spectrophotometer was used for UV–vis absorption. A fluorescence spectrophotometer F-4500 (Hitachi High-Technologies Corporation) was used to analyse fluorescence excited spectra. Cyclic voltammetric measurements were performed

on an LK3200A electrochemical workstation (Lanlike Chemistry and Electron High Technology Corporation, Tianjin, China), using 1.0 mm dye solution in DMF at a scan rate of 50 MV s^{-1} and 0.1 M tetrabutylammoniumhexafluorophosphate as the supporting electrolyte.

2.3 *Computational study*

All the molecular structures in the ground state were first optimized by using the DFT/B3LYP method at the 6-31G(d,p) basis set to obtain the energy minima geometries. Then theoretical electronic absorption spectra of the optimized structures were predicted based on the TDDFT/B3LYP method at the 6-311G(d,p) basis set. Quantum chemical calculations were performed using the Gaussian-09 software package on the cloud computing platform of BUCT, and the calculation results were visualized using the Gaussian View-5.0 program on a personal computer.

2.4 *Synthesis*

2.4a *Synthesis of MEC*: MIC (2.93 g, 0.01 mol), PPh$_3$ (0.13 g, 0.50 mmol), CuI (0.10 g, 0.50 mmol) and Pd(PPh$_3$)$_2$Cl$_2$ (0.02 g, 0.03 mmol) were added in a tri-necked flask with 90 ml DMF and 30 ml TEA. Nitrogen (N$_2$) was used to deaerate the solution in lieu of 30 min and then the solution was gradually warmed up to 55°C. Subsequently heating it for 30 min more the temperature was enhanced to 85°C. After adding 3-ethynyl-9*H*-carbazole (2.48 g, 0.013 mol), the reaction concoction was kept on a stirrer for an additional 3.5 h under a N$_2$ atmosphere. TLC was used to perceive the reaction timely till the end of the process. Salts were removed by filtration and the filtrate decanted into a saturated solution of ammonium chloride (NH$_4$Cl) (aq) and DCM (CH$_2$Cl$_2$) used to extract it. The organic solvents were separated by using a rotary evaporator to obtain a solid crude product of MEC which was further subjected to the column chromatography purification process (PE/DCM (8/1–2/1)), to obtain MEC (2.99 g, yield: 78%) as a pure yellow solid. MP: 230–235°C. ^{1}H NMR (400 MHz, DMSO-d_6) δ (ppm): 11.52 (s, 1H), 8.45 (m, 2H), 8.27 (m, 2H), 7.67 (m, 4H), 7.57 (m, 4H), 7.27 (m, 2H), 4.49 (m, 2H), 1.35 (m, 3H). ^{13}C NMR (100 MHz, DMSO-d_6) δ (ppm): 140.11, 139.94, 139.24, 138.97, 128.79, 128.68, 126.23, 126.06, 123.46, 123.39, 122.61, 122.35, 121.96, 121.74, 120.73, 120.55, 119.21, 119.01, 112.98, 112.73, 111.31, 111.14, 109.49, 109.32, 88.97, 88.59, 37.09, 13.70. IR (KBr; ν (cm^{-1})): 3414 (Ar-H), 2321 (–C≡C–), 1603 (–C≡C–). ^{1}H NMR, ^{13}C NMR and IR graphs are presented in supporting information as figure S1, S5 and S9. **MS**. HRMS (MALDI-TOF) m/z calcd for C$_{28}$H$_{20}$N$_2$ 385.1; found: 385.1 [M$^+$].

2.4b *Synthesis of DEC*: DEC was prepared by using the procedure alike to MEC, except that DIC was used instead of MIC. Yield: 76%. MP: 260–265°C. ^{1}H NMR (400 MHz, DMSO-d_6) δ (ppm): 11.77 (s, 1H), 8.52 (m, 4H), 8.28 (m, 2H), 7.67

(m, 10H), 7.52 (m, 2H), 7.27 (m, 2H), 4.48 (m, 4H), 1.35 (m, 6H). ^{13}C NMR (100 MHz, DMSO-d_6) δ (ppm): 139.95, 139.66, 139.02, 129.34, 128.85, 126.25, 123.75, 123.51, 122.37, 122.22, 121.74, 120.75, 119.23, 113.35, 112.89, 111.62, 109.51, 109.33, 88.90, 88.87, 37.10, 13.70. IR (KBr; ν (cm^{-1})): 3398 (Ar-H), 2359, 2344 (–C≡C–), 1603 (–C=C–). ^{1}H NMR, ^{13}C NMR and IR graphs are presented in supporting information as figure S2, S6 and S10. **MS**. HRMS (MALDI-TOF) m/z calcd for $C_{44}H_{31}N_3$ 601.2; found: 601.2 [M$^+$].

2.4c *Synthesis of MPC*: MPC was prepared by using the procedure alike to MEC, except that PA (1.02 g, 0.01 mol) was used instead of 3-ethynyl-9H-carbazole. Yield: 78%. MP: 230–235°C. ^{1}H NMR (400 MHz, DMSO-d_6) δ (ppm): 11.52 (s, 1H), 8.40 (s, 1H), 8.21 (d, J = 7.5 Hz, 1H), 7.57 (m, 9H), 7.21 (m, 1H). ^{13}C NMR (100 MHz, DMSO-d_6) δ (ppm): 140.10, 139.51, 131.06, 128.82, 128.69, 128.15, 126.14, 123.76, 123.06, 122.58, 121.91, 120.57, 119.09, 111.89, 111.33, 111.17, 91.15, 87.16. IR (KBr; ν (cm^{-1})): 3404 (Ar-H), 2211 (–C≡C–), 1593 (–C=C–). ^{1}H NMR, ^{13}C NMR and IR graphs are presented in supporting information as figure S3, S7 and S11. **MS**. HRMS (MALDI-TOF) m/z calcd for $C_{20}H_{13}N$ 268.1; found: 268.0 [M$^+$].

2.4d *Synthesis of DPC*: DPC was prepared by using the procedure similar to MPC, except that DIC was used instead of MIC. Yield: 76%. MP: 265–270°C. ^{1}H NMR (400 MHz, DMSO-d_6) δ (ppm): 11.79 (s, 1H), 8.48 (s, 2H), 7.64 (m, 8H), 7.48 (m, 6H). ^{13}C NMR (100 MHz, DMSO-d_6) δ (ppm): 139.93, 131.12, 129.50, 128.72, 128.25, 124.16, 122.94, 122.15, 112.60, 111.67, 90.95, 87.45. IR (KBr; ν (cm^{-1})): 3411 (Ar-H), 2211, 2356 (–C≡C–), 1593 (–C=C–). ^{1}H NMR, ^{13}C NMR and IR graphs are presented in supporting information as figure S4, S8 and S12. **MS**. HRMS (MALDI-TOF) m/z calcd for $C_{28}H_{17}N$ 368.1; found: 368.1 [M$^+$].

2.5 *Photopolymerization*

Nicolet 5700 instrument (Thermo Electron Corporation, Waltham, MA) was used to obtain IR spectra. 1.8 mm chunky plastic frames with the centre of 10 mm diameter were used to photocure the sample. The frames were braced between two glass slides. Halogen light at 365 nm was employed to illuminate the samples. The distance was set by 15 cm between the sample and irradiation light, and 2 and 30 mW cm^{-2} were set as light intensities, respectively. The NIR test was run thrice for each sample. By controlling the curing light manually the samples were permeated at varying time intervals. Spectra were recorded right after every single revealing interval at the time of compilation of the uncured resin NIR spectrum [16,23]. As Stansbury and Dickens described the absorption band for double-bond conversion profiles situated at 6165 cm^{-1} were calculated by using

$$\text{Conversion}\% = \left[1 - \frac{S_t}{S_0}\right] \times 100\%, \qquad (1)$$

where S_t is the area of double-bond absorbance peak and S_0 is the primary area of the double-bond absorbance peak [24]. To resolve the epoxy conversion, the peak situated at 6075 cm^{-1} was calculated [25]. The epoxy conversion was premeditated by equation (1): here we consider S_t as the area of the epoxy C–H characteristic absorbance peak and S_0 as the primary area of the epoxy C–H characteristic absorbance peak.

2.6 *Electrochemical analysis*

Cyclic voltammetric measurements were performed on an LK3200A electrochemical workstation, using 1.0 mM dye solution in DMF at a scan rate of 50 mV s^{-1} and 0.1 M tetrabutylammoniumhexafluorophosphate as the supporting electrolyte. Before measurement, each solution was nitrogen bubbled for 30 min. Glassy carbon, standard calomel electrode (SCE) and a platinum wire were used as working, reference and auxiliary electrodes, respectively.

3. Results and discussion

3.1 *Synthesis*

Sonogashira cross-coupling reaction was used to synthesize key products named as MEC, DEC, MPC and DPC in the mixture of ethynylated carbazole and ethynylated benzene with MIC or 3,6-iodo-9H-carbazole using PdCl$_2$(PPh$_3$)$_2$ as a catalyst. Figures S1–S4 show the ^{1}H NMR spectra of the synthesized alkynylcarbazole compounds, and it is noted from the figures that the chemical shift δ =1–1.5 ppm were assigned
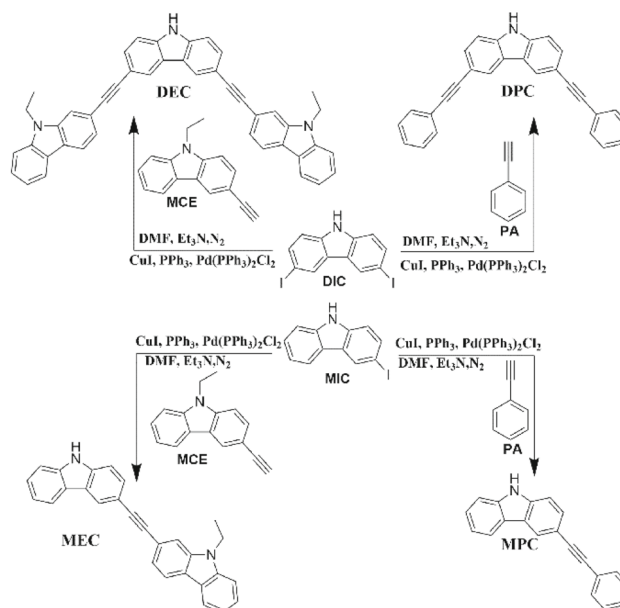
Scheme 1. Synthesis route for conjugated alkynylcarbazole dyes.

Table 1. Electronic transition of alkynylcarbazole in the gas and solution phases.

Alkynylcarbazole	Experimental data		Calculated data				
	λ_{max} (nm)	$\varepsilon \times 10^4$ (M^{-1} cm^{-1})	States	E (eV)	λ (nm)	f_{os}	HOMO $\rightarrow$ LUMO
MEC	304	9.4	S1	3.5406	350.18	0.1482	101 $\rightarrow$ 102
			S3	3.7272	332.64	1.2579	101 $\rightarrow$ 104
DEC	304	9.7	S1	3.3988	364.79	1.7542	158 $\rightarrow$ 159
			S5	3.7026	334.86	0.4291	157 $\rightarrow$ 160
MPC	299	6.9	S1	3.7279	332.58	0.1639	70 $\rightarrow$ 72
			S2	3.8451	322.45	0.8147	70 $\rightarrow$ 71
DPC	311	6.3	S1	3.5191	352.32	0.9718	96 $\rightarrow$ 97
			S4	3.9441	314.35	0.6463	95 $\rightarrow$ 98
			S5	4.1312	300.12	0.8483	95 $\rightarrow$ 97
EtCz	294	2.1	—	—	—	—	—

to hydrogen of the CH_3 group and the chemical shifts for NCH were found in the range of $\delta = 4$–5 ppm in the cases of MEC and DEC. The chemical shifts $\delta = 11.0$–12.0 ppm show the presence of N–H (aliphatic) hydrogen, while the chemical shifts of all other conjugated protons occurred in the range of $\delta = 7$–9 ppm. Figures S9–S12 show IR spectra, and an intense peak for N–H was shown in the range of 3395–3415 cm^{-1}, a very insubstantial peak of the C≡C stretching was located at 2211–2344 cm^{-1} and for other conjugated C=C bonds a quite clear peak was seen in the range of 1593–1603 cm^{-1}. It was confirmed by characterization that the products were synthesized accurately. The way of synthesis for these four dyes is shown in scheme 1.

3.2 *Optical analysis and DFT calculations*

The UV–vis absorption spectra of alkynylcarbazoles were observed in THF with a concentration of 1×10^{-5} and 1×10^{-3} mol l^{-1}. *N*-Ethylcarbazole (EtCz) was taken as a reference compound for comparison with the synthesized compounds. The predicted ultraviolet spectra of these compounds were obtained by theoretical calculations. The 50 singlet–singlet excitations of every compound were measured by a TD/DFT procedure initiated by optimized geometry. The absorption of interest with a wavelength $(\lambda) > 300$ nm and an oscillator strength $(f_{os}) > 0.1$ is listed in table 1. For elaborating the theoretical spectra, the full-width at half-maximum value of the spectrum was set at 0.3 eV by Multiwfn to clearly define the contribution of every excited state to the spectrum.

Figure 2a shows the UV–vis absorption spectra of alkynyl-carbazole dyes in THF ($M = 1 \times 10^{-5}$ mol l^{-1}). Every conjugated alkynylcarbazole dye exhibits a wide absorption band in the range of 300–400 mm. EtCz has the lowest absorption in comparison with the synthesized alkynylcarbazole compounds. Figure 2b shows the UV–vis absorption spectra of alkynylcarbazole dyes in THF ($M = 1 \times 10^{-3}$ mol l^{-1}), which showed a red-shift phenomena of the synthesized alkynylcarbazole compounds by enhancing the conjugation compared with EtCz in the range of 350–450 nm.

Moreover, it was also observed that by switching moieties from PA to carbazoleacetylene also can cause an obvious red shift in the absorption bands by the enhancement in conjugation.

Furthermore, figure 2c shows the theoretical UV spectra of alkynylcarbazole compounds, and it shows that the maximum λ of the range of alkynylcarbazole compounds is ∼330–370 mm, corresponding to the $\pi \rightarrow \pi^*$ and $n \rightarrow \pi^*$ electron transitions. The highest λ value of 364 nm, which was observed in the DEC, was mostly ascribed to the strong electron-accepting group, whereas MPC presented the lowest λ_{max} value among the other groups because of the high-energy gap between the highest occupied molecular orbital (HOMO) and the lowest unoccupied molecular orbital (LUMO). The maximum absorption peak in DEC can be observed at 364 nm because of its oscillator strength of 1.7542, indicating that the absorption probability in this area was extremely high. However, the peak in the experimental spectrum was not the highest because the theoretical spectrum calculations were confined to the gaseous equivalent, whereas the observations originated from the solution state (figure 3).

In summary, the comparison shows that the λ_{max} of the theoretical ultraviolet spectra was matched well with the experimental spectra. The obtained experimental data showed similarity by taking MEC as a pattern with 350 nm transition in the calculated gas phase. Table 1 illustrates the data obtained from all experimental and theoretical analyses of all alkynylcarbazole compounds. The geometrical analysis of all obtained dyes is shown in figure 3 and their HOMO and LUMO values are exhibited in table 2.

3.3 *Fluorescence spectroscopic study (quantum yield)*

Fluorescence spectroscopy was conducted using the THF solution at a concentration of 1.0×10^{-5} M to obtain information regarding the values of quantum yield and fluorescence emission spectra for alkynylcarbazole dyes. Figure 4 shows the fluorescence emission spectra of all dyes, and table 3 shows the data of emission spectra and quantum yield.
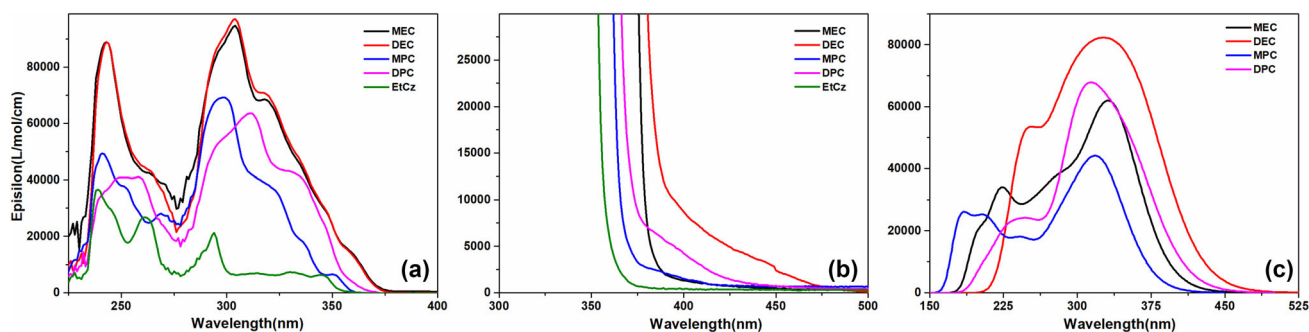
Figure 2. Comparative UV spectra of experimental and theoretical analysis: (**a**) UV–vis absorption spectra of alkynylcarbazole dyes in THF, $M = 1 \times 10^{-5}$ mol l^{-1}; (**b**) UV–vis absorption spectra of alkynylcarbazole dyes in THF, $M = 1 \times 10^{-3}$ mol l^{-1} and (**c**) theoretical UV spectra by the TD/DFT procedure.
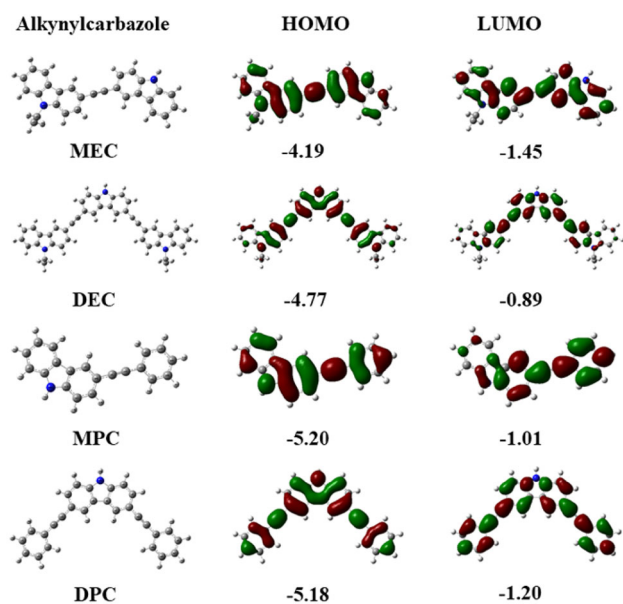

Figure 3. Geometrical analysis, HOMO and LUMO structures of alkynylcarbazole compounds.

Table 2. Data of the HOMO to LUMO transitions of alkynylcarbazole compounds.

Dyes	HOMO (eV)	LUMO (eV)	E_{gap} (eV)
MEC	−4.19	−1.45	2.74
DEC	−4.77	−0.89	3.88
MPC	−5.20	−1.01	4.19
DPC	−5.18	−1.20	3.98

These alkynylcarbazole dyes exhibit the blue-violet fluorescence emission of 350–450 nm. The largest emission peaks exhibited a red shift by adding the numbers of conjugated acetylene structures and the degree of π delocalization in dyes. Moreover, fluorescence spectroscopy shows that the double-substitute compounds of DEC and DPC exhibit maximum emissions of ∼395 and 387 nm. The large
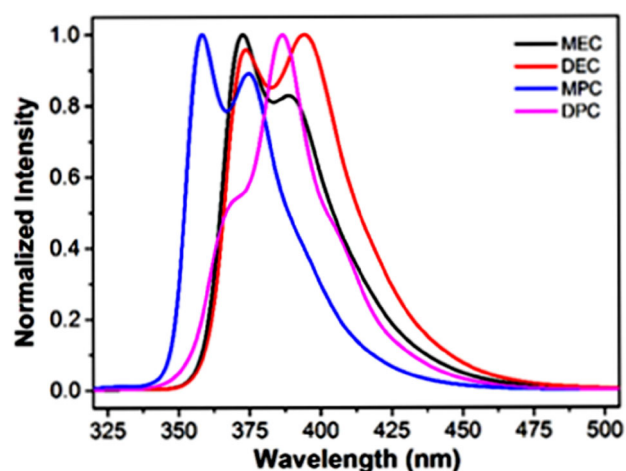

Figure 4. Fluorescence emission spectra of alkynylcarbazole dyes in THF solution ($M = 1 \times 10^{-5}$ mol l^{-1}).

Stokes' shift shows that the excited states of alkynylcarbazole compounds exhibit superior polarity and redistribution in the excited state of the intra-molecular charge. Furthermore, the values of emission appeared to be in sequence with theoretical electron transitions; thus, the increased absorption affects emission. DPC exhibits higher fluorescence quantum yields than the other compounds.

3.4 *Electrochemical study*

Electrochemical analysis was conducted to check and further extend the electron transfer properties and redox potentials of conjugated alkynylcarbazole compounds for electron transfer photosensitizers of onium salts. Figures S13–S16 and table 4 show the CV curves for MEC, DEC, MPC and DPC and electrochemical data, respectively. The calculated free-energy change ΔG_{et} shows that the dye/ONI electron transfer reaction satisfactorily corresponds to the redox characteristics of reactants. The photoinduced electron transfer route was thermodynamically acceptable for these complexes, as found by the ΔG_{et} negative values.

Table 3. Fluorescence spectra analysis of alkynylcarbazole compounds.

Alkynylcarbazole dyes	λ_{max} (nm)	λ_{em} (nm)	Stokes' shift (nm)	Φ
MEC	304	373	69	0.49
DEC	304	395	91	0.44
MPC	299	359	60	0.53
DPC	311	387	76	0.54

Table 4. Data of the electrochemical analysis of alkynylcarbazoles.

| Dyes	E_{OX} (V)	E_{00} (eV)	ΔG_{et} (eV)
MEC	1.31	3.63	−1.67
DEC	0.38	2.85	−1.82
MPC	0.46	2.91	−1.81
DPC	0.93	2.86	−1.28

3.5 *Photopolymerization*

The photopolymerization experiment was adopted as suggested in previous work in the literature [7,8,26]. Carbazole was used as a reference, and ONI was tested separately to evaluate the properties of photopolymerization in the presence of a halogen lamp at 365 nm. The cationic polymerizations of bisphenol-A epoxy resin A (DGEBA) and free-radical polymerization of TPGDA with the addition of alkynylcarbazole dyes and ONI were conducted. Figure 5a and b show the time-dependent double-bond conversion of photocurable resin films from TPGDA and time-dependent epoxy conversion of photocurable resin films from DGEBA, respectively.

Figure 5 shows that the dye/ONI can photoinitiate the photopolymerization of TPGDA and DGEBA under the halogen lamp atmosphere, whereas table 5 displays the comparative conversion rate at different time gaps for double-bond and epoxy conversion.

Figure 5a shows that the double-bond conversion for Cz exhibits zero efficiency, and that for ONI shows under 30% conversion, whereas the main compounds of MEC/ONI, DEC/ONI and DPC/ONI systems offer analogous efficiency
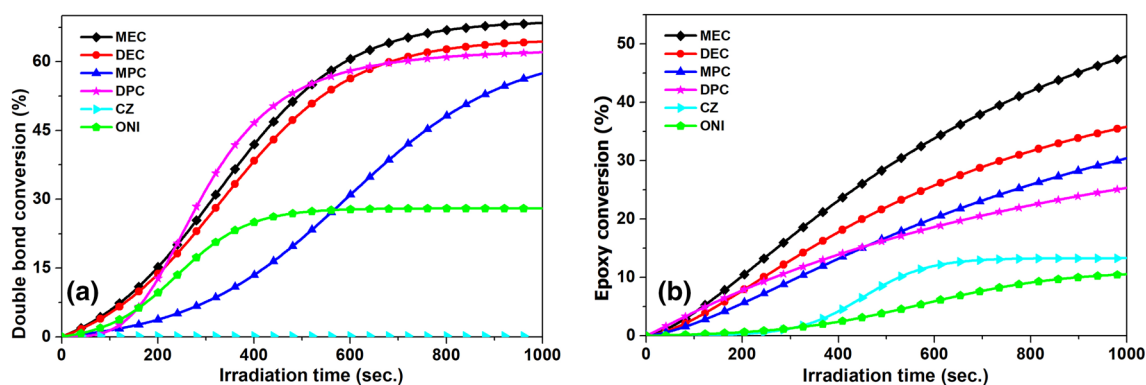
Figure 5. Photopolymerization data on the basis of free-radical and cationic photopolymerization under a halogen lamp: (**a**) TPGDA: 100 wt%; ONI: 2.0 wt%; dye: 0.2% and (**b**) DGEBA: 100 wt%; ONI: 2.0 wt%; dye: 0.2%.

Table 5. Data of the electrochemical analysis of alkynylcarbazoles.

Alkynylcarbazole compounds	Double-bond conversion (%)			Epoxy conversion (%)		
	200 s	300 s	C_f	200 s	300 s	C_f
MEC	15.2	28.1	68.4	10.5	17.2	47.9
DEC	13.7	25.5	64.3	7.9	13.2	36.1
MPC	3.7	7.6	57.4	5.6	9.6	30.7
DPC	12.7	32.1	62.0	7.9	11.2	25.6
ONI	9.6	19.0	28.0	0.63	1.3	10.6
Cz	0.18	0.18	0.18	0.62	1.3	13.2

and additional effectiveness compared with the MPC/ONI systems because MPC exhibits the lowest absorption in the visible region among these alkynylcarbazole dyes.

In the cationic photopolymerization in figure 5b, Cz and ONI exhibit extremely low efficiency on an individual basis, but the efficiency order of photoinitiating systems appears as MEC/ONI>DEC/ONI>MPC/ONI>DPC/ONI. MEC/ONI and DEC/ONI systems are more capable than DPC/ONI and MPC/ONI systems because MEC and DEC possess more carbazole moieties and conjugation and exhibit higher absorption than DPC and MPC.

4. Conclusion

A group of dyes containing alkynylcarbazole was investigated on the basis of extending conjugation by exchanging carbazolylacetylene to single and double substitutes. UV–vis spectroscopy and TD/DFT analysis show that these dyes exhibit a wide absorption band in the range of 300–400 nm, and the maximum λ of these molecules ranges from ∼330–370 mm, corresponding to $\pi \rightarrow \pi^*$ and $n \rightarrow \pi^*$ electron transitions. Conjugation extension results in a red shift in the absorption bands. The dye/ONI electron transfer reaction satisfactorily corresponds to the redox characteristics of reactants, as confirmed by the free-energy change ΔG_{et}. The photo-induced electron transfer route is thermodynamically acceptable for these complexes, as evidenced by ΔG_{et} negative values. Through photopolymerization, compounds with strong absorption in DEC and MEC are more efficient than compounds with low absorption in MPC and DPC. This work also illustrates that the increase in conjugation may change optical properties. Moreover, these dyes are beneficial for visible-light-induced photopolymerization by halogen light.

Acknowledgements

References

[1] Minezawa N 2015 *Chem. Phys. Lett.* **622** 115
[2] Sacarescu L, Fortuna M, Soroceanu M, Cojocaru C, Sacarescu G, Simionescu M *et al* 2015 *Silicon* **7** 343
[3] Crivello J V and Jiang F 2002 *Chem. Mater.* **14** 4858
[4] Crivello J V and Jang M 2005 *J. Macromol. Sci. Part A Pure Appl. Chem. A* **42** 1
[5] Xiao P, Lalevee J, Zhao J and Stenzel M H 2015 *Macromol. Rapid. Commun.* **36** 1675
[6] Zhang J, Campolo D, Dumur F, Xiao P, Gigmes D, Fouassier J P *et al* 2016 *Polym. Bull.* **73** 493
[7] Zhou T F, Ma X Y, Han W X, Guo X P, Gu R Q, Yu L J *et al* 2016 *Polym. Chem.* **7** 5039
[8] Wang M, Ma X, Yu J, Jia X, Han D, Zhou T *et al* 2015 *Polym. Chem.* **6** 4424
[9] Zahlou A, Sadiki Y, Bejjit L, Haddad M, Hamidi M and Bouachrine M 2014 *J. Mater. Environ. Sci.* **5** 532
[10] Sathiyan G, Sivakumar E K T, Ganesamoorthy R, Thangamuthu R and Sakthivel P 2016 *Tetrahedron Lett.* **57** 243
[11] Al Mousawi A, Garra P, Dumur F, Bui T T, Goubard F, Toufaily J *et al* 2017 *Molecules* **22** 1
[12] Al Mousawi A, Dumur F, Garra P, Toufaily J, Hamieh T, Graff B *et al* 2017 *Macromolecules* **50** 2747
[13] Zhang J, Campolo D, Dumur F, Xiao P, Gigmes D, Fouassier J P *et al* 2016 *Polym. Bull.* **73** 493
[14] Li G L, Liu J Q, Zhao B D and Wang T 2013 *Spectrochim. Acta A Mol. Biomol. Spectrosc.* **104** 287
[15] Bourass M, Touimi B A, Benzakour M, Mcharfi M, Jhilal F, Serein S F *et al* 2017 *J. Saudi Chem. Soc.* **21** 563
[16] Madkour L H, Kaya S, Kaya C and Guo L 2016 *J. Taiwan Inst. Chem. Eng.* **68** 461
[17] Stalindurai K, Gokula K K, Nagarajan E R and Ramalingan C 2017 *J. Mol. Struct.* **1130** 633
[18] Shao J, Huang Y and Fan Q 2014 *Polym. Chem.* **5** 4195
[19] Sipani V and Scranton A B 2004 *Encycl. Polym. Sci. Technol.* (New York: John Wiley & Sons, Inc.)
[20] Tucker S H 1926 *J. Chem. Soc.* **129** 546
[21] Kumchoo T, Promarak V, Sudyoadsuk T, Sukwattanasinitt M and Rashatasakhon P 2010 *Chem. – Asian J.* **5** 2162
[22] Kato S I, Noguchi H, Kobayashi A, Yoshihara T, Tobita S and Nakamura Y 2012 *J. Org. Chem.* **77** 9120
[23] Chao P, Gu R, Ma X, Wang T and Zhao Y 2016 *Polym. Chem.* **7** 5147
[24] Stansbury J W and Dickens S H 2001 *Dent. Mater.* **17** 71
[25] Jiang B and Huang Y D 2008 *Composites Part A* **39** 712
[26] Abro H A, Zhou T, Han W, Xue T and Wang T 2017 *RSC Adv.* **7** 55382